CrossMark

REVIEW PAPER

Review: on rare-earth perovskite-type negative electrodes in nickel–hydride (Ni/H) secondary batteries

John Henao[1] · Lorenzo Martinez-Gomez[1]

Abstract Rare-earth perovskites-type oxides are compounds with the general formula ABO_3. There are many industrial and research applications related to their properties such as photocatalytic activity, magnetism, or pyro-ferro and piezo-electricity, and interest in these compounds in the field of energy storage and conversion is growing. Rare-earth perovskite-type oxides may be used in nickel–metal hydride (Ni/MH) battery technology because these materials may store hydrogen in strong alkaline environments, and also because of their abundance and low cost. In this review, the use of rare-earth perovskite-type oxides in Ni/MH batteries is described, starting from their crystalline structure and production methods. In each category, a description concerning the latest advances and future research direction is presented. Electrochemical performance of the perovskite-type electrodes is reviewed extensively. In addition, various strategies for enhancing their hydrogen storage capacity as a negative electrode in hydrogen batteries are discussed. Drawbacks and challenges of this technology are also presented.

✉ John Henao
  jhenao.icf.unam@gmail.com

[1] Instituto de Ciencias Físicas, Universidad Nacional
  Autónoma de México (UNAM), Avenida Universidad s/n,
  62210 Cuernavaca, Morelos, Mexico

مدينة الملك عبدالعزيز
KACST للعلوم والتقنية

Springer

Graphical Abstract

Review: On rare-earth perovskite-type negative electrodes in Nickel-hydride (Ni/H) secondary batteries

Nickel-metal hydride battery

Perovskite structure

Electrochemical performance
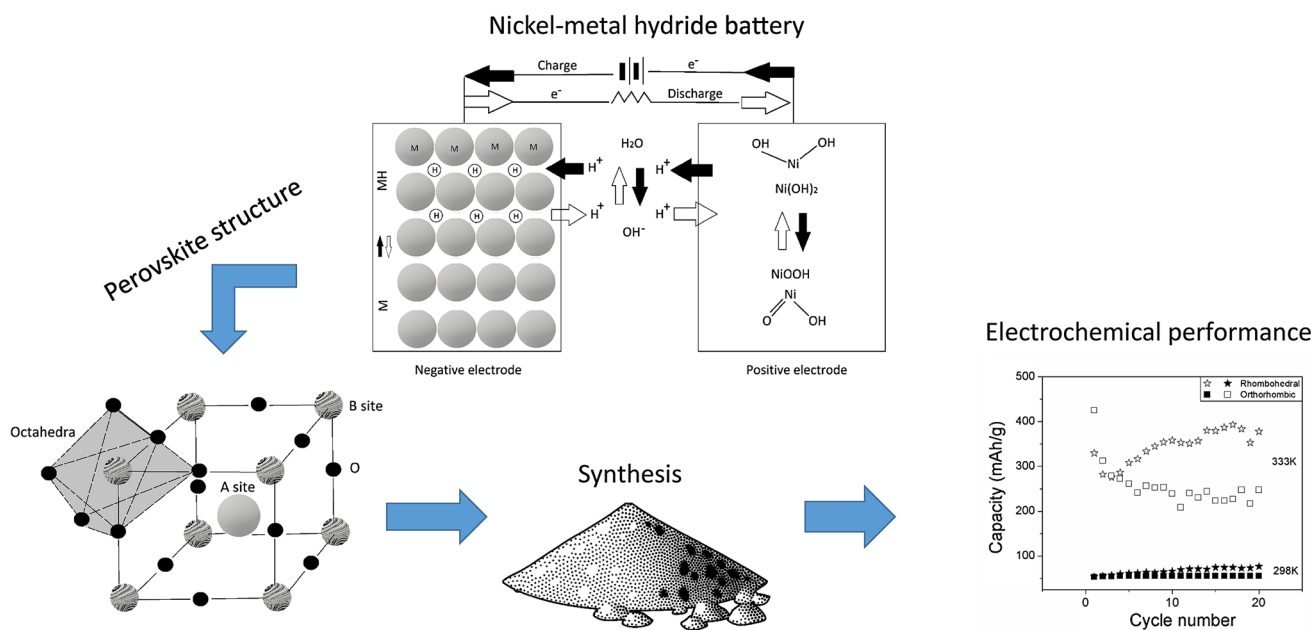
Keywords Metal hydride (MH) · Perovskites · Rare earth · Rechargeable battery · Hydrogen
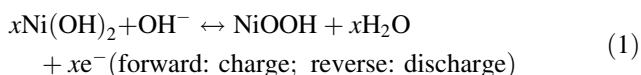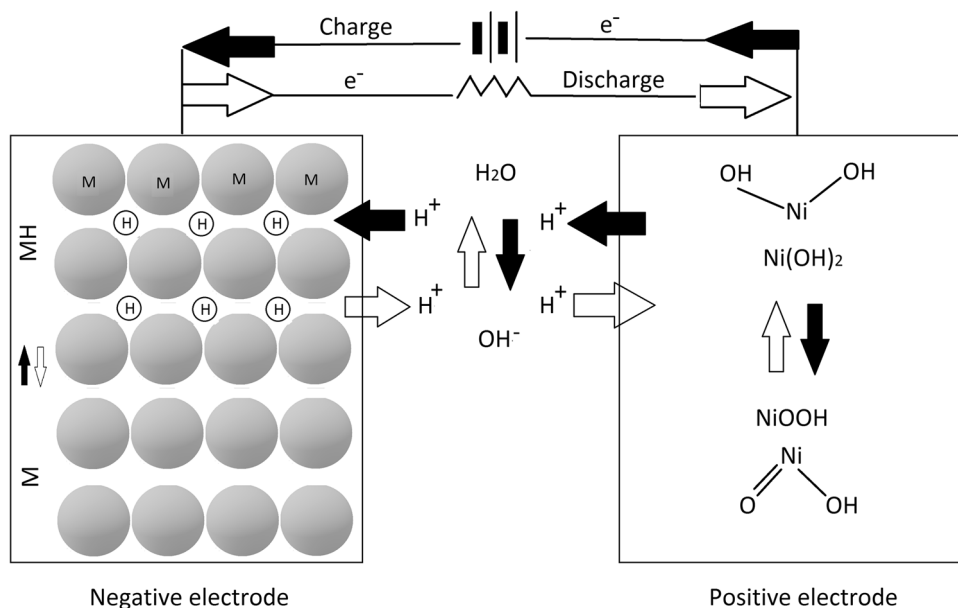
Introduction

The development of renewable sources, in the electronic and automotive industry have led engineering to limit its impact on the environment and transform energy associated technologies into sustainable and environmentally friendly devices. In the fields of energy storage and conversion, rechargeable batteries have experienced constant advances in their architecture and materials to get a better performance with a lower environmental cost [1–3]. Among the various rechargeable battery technologies, nickel–metal hydride (Ni/MH) and lithium ion (Li-ion) batteries have experienced continuous development in the last decades. The Ni/MH battery has a relatively low nominal voltage value (1.2 V) with a voltage window ranging from 0.6 to 1.5 V when compared to the rival Li-ion battery (nominal voltage 3.6 V with a voltage window from 3.0 to 4.2 V). Having a lower voltage means that more Ni/MH cells connected in series in a battery pack are required to ach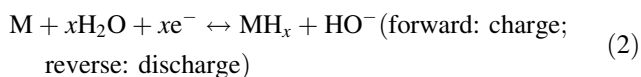ieve a pre-determined pack voltage (for instance, three Ni/MH cells instead of one Li-ion cell for a pack voltage of 3.6 V). The Ni/MH battery also has a relatively high energy density (Wh L^{-1}) but a rather low specific energy (Wh kg^{-1}) when compared to the Li-ion battery as a result of the high density of its active materials in the anode (nickel-based alloys versus graphite) [4]. Thus, Ni/MH batteries are widely used in stationary applications, consumer electronics, power tools, hybrid and full electric road and rail vehicles because of its durability, abuse tolerance, compact size, and environmental friendliness [5–8]. On the other hand, Li-ion batteries are commonly used in applications where strict requirements in power and energy are needed, such as in electric vehicles and mobile phones [4, 9].

The Ni/MH battery is a reversible electrochemical device that allows to store and produce electrical energy by means of electrochemical reactions. These reactions occur at the surface of active materials (or electrodes) in contact with an alkaline electrolyte, Fig. 1. The active material used in the positive electrode (cathode) of these batteries is the $Ni(OH)_2$ compound. During charge, this active material experiences +2/+3 oxidation state change promoted by the electrochemical reaction [10, 11]. The following half-cell electrochemical reaction takes place at the cathode:
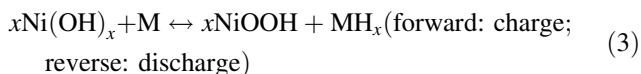
Fig. 1 Schematic diagram of the operation of a Ni/MH cell

Negative electrode   Positive electrode

$$x\text{Ni(OH)}_2 + \text{OH}^- \leftrightarrow \text{NiOOH} + x\text{H}_2\text{O}$$
$$+ x\text{e}^- \text{(forward: charge; reverse: discharge)} \quad (1)$$

As a result, protons released from the active material move to its surface and recombine with hydroxide ions in the electrolyte. On the other hand, in the negative electrode (anode), the active material is a special kind of alloy known as hydrogen storage alloy (or metal hydride (MH) alloy) that is capable to store hydrogen in a reversible way [12]. During charge, the applied voltage splits water molecules into hydroxide ions and hydrogen protons. As a result, the reduction of water allows hydrogen protons to be in contact with the hydrogen storage alloy. Protons enter then into the bulk of the alloy to form a MH driven by the voltage and diffusion caused by the concentration gradient [12, 13]. The half-cell electrochemical reaction at the anode is:

$$\text{M} + x\text{H}_2\text{O} + x\text{e}^- \leftrightarrow \text{MH}_x + \text{HO}^- \text{(forward: charge;}$$
$$\text{reverse: discharge)} \quad (2)$$

Therefore, the overall reaction for the battery is:

$$x\text{Ni(OH)}_x + \text{M} \leftrightarrow x\text{NiOOH} + \text{MH}_x\text{(forward: charge;}$$
$$\text{reverse: discharge)} \quad (3)$$

In the negative electrode, adsorption/absorption of hydrogen is crucial for the operation of the cell. A good hydrogen storage electrode material must have the following properties [14, 15]: (1) catalyst for hydrogen atom, (2) corrosion resistance, (3) reversible hydrogen storage capacity, (4) good operation in a wide range of temperatures, (5) suitable hydrogen equilibrium pressure and (6) low cost. Currently, Ni/MH batteries are equipped with negative electrodes which are usually fabricated from intermetallic

compounds. These alloys are able to absorb hydrogen within its structure, leading to the formation of metal hydrides. Among several families of intermetallic compounds (AB, AB_2, A_2B, A_2B_7 and AB_5; where A: is an element with high affinity for hydrogen ions, and B: is an element with a low affinity for hydrogen), the intermetallic AB_5-type compounds, specially the $LaNi_5$-based alloys, are currently the most common compositions in commercial Ni/MH batteries (typical composition: $MmNi_{3.55}Co_{0.75}Mn_{0.4}Al_{0.3}$; where Mm: is called mischmetal or a mixing of rare-earth elements, usually composed by $La_{0.62}Ce_{0.27}Pr_{0.03}Nd_{0.08}$) [13, 16].

The AB_5-type hydrogen storage alloys are very convenient due to their clean characteristics and good performance in Ni/MH batteries [17]. However, the high production cost and limited capacity (330 mAhg^{-1}) of these compounds slows down their application in commercial devices. Recently, the substitution of elements such as La, Nd, Mn, in AB_5-type alloys and the total replacement of the La-based alloys by others intermetallic systems (Mg-based and Ti-based) have been alternatives proposed for cost reduction [18–20]. However, further work should be carried out to improve stability and performance of these alloys at different operational conditions in Ni/MH batteries.

In the last decade, rare-earth (RE) perovskite-type oxides (ABO_3), which are reported herein as hydrogen uptake materials [21–28], have been regarded to be one of the valuable alternatives as negative electrode materials in Ni/MH batteries. This fact is attributed to the lower cost of perovskite-type oxides than conventional intermetallic alloys, due to its thermally stability, abundance, and

comparatively active behavior [27–29]. RE-perovskite-type oxides are known not only to present proton conductivity at high temperatures and under hydrogen atmospheres, but also to have higher hydrogen solubility than other metal oxides. Due to its properties, RE-perovskite-type oxides have become widely used in practical applications such as fuel cells, catalyst, corrosion inhibition and electrochemical capacitors [30–33]. However, as potential anode materials for hydrogen secondary batteries, RE-perovskite-type oxides are still a research field under development. This article is focused on reviewing RE-perovskite-type oxides as alternative negative electrodes for Ni/MH batteries and gives the basis for the future research directions in this field. Structure and synthesis methods are also reviewed.

Perovskite structure

It is well-known that perovskite-type oxides constitute one of the most important and widely studied families of oxide compounds due to its interesting dielectric and ferroelectric properties, magnetic behavior, electronic and ionic conductivity, and superconductivity [30, 34, 35]. Their flexibility in accommodating a broad range of atomic substitutions provides to these oxides a wide variety of properties while keeping its basic structure unchanged.

Ideal perovskite-type oxides exhibit a crystal cubic structure with space group Pnma (Pm3–m cubic system) described by the general formula ABO_3 (where A: is a rare or alkaline earth metal and B: is a first-row transition metal), wherein cations with a large ionic radius coordinate to 12 oxygen atoms and occupy A-sites and cations with a smaller ionic radius are 6 coordinate and occupy B-sites [36, 37], Fig. 2.

Unlike ideal cubic perovskite structures, real perovskite ABO_3 oxides exhibits lattice distortions of various degrees (octahedra are tilted around its center), thereby resulting in the transformation of crystal phases in the
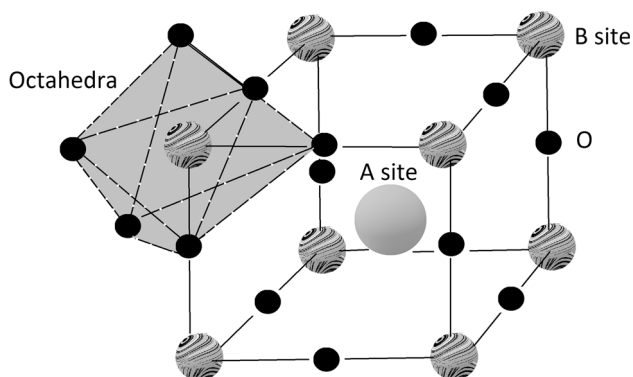
following sequences: orthogonal, rhombohedral, tetragonal, monoclinic, and triclinic phase, depending on the details of the octahedral rotations. Interestingly, rotations of the oxygen octahedra have an important impact on the crystal field, and thus it changes the dipole and electronic band structures, thereby influencing its physical and chemical behavior [37, 38]. Table 1 summarizes experimentally determined RE-perovskite type structures in early works.

Usually, the ABO_3 structure is partial substituted by cations at the A and B-sites to promote octahedral rotation, improving ionic conductivity and hydrogen catalytic activity. For RE-perovskite-type oxides, the most symmetric structure observed is rhombohedral R3c (i.e., $La_{1-x}Sr_xFeO_3$) [58]. These oxides involve a distortion of the ideal cubic structure due to a rotation of the BO_6 octahedra and a displacement of the A cation with respect to its initial position in the cubic structure. The rhombohedral structure from $La_{1-x}Sr_xFeO_3$ has been one of the studied structures in Ni/MH batteries [59], nevertheless, further studies must be carried out to determine which of the lattice distortions are the most favorable for electrochemical hydrogen insertion in Ni/MH batteries.

Synthesis of rare-earth perovskite-type oxides for applications in Ni/MH batteries

Previous studies regarding RE-perovskite-type oxides in the field of Ni/MH batteries have involved a number of synthesis routes. These routes include the solid-state reaction, the glycine-nitrate method, and the sol–gel technique. The solid-state reaction method is a conventional technique for the synthesis of ceramic compounds. It consists in the mechanical mixing of nearly pure oxide powders (99% purity), carbonates or salts, followed by heat treatment at high temperatures, typically around 1500 K. This process is often carried out for 8–24 h to allow the rearrangement of cations to form the perovskite-type structure [28, 60–62]. The reactions tend to occur at the interface of the mixed solids as ions diffuse from the bulk to the interface between particles. This method is known to produce a dense material [60, 61]. Following heat treatment, the material is milled to obtain micrometric powders. For instance, Kim et al. [63] prepared polycrystalline $BaZr_{0.65}Ce_{0.2}Y_{0.1}Rb_{0.05}O_{3-\delta}$ samples by the conventional solid-state process. They started from high-purity powders (99.9% purity) of $BaCO_3$, CeO_2, ZrO_2, Y_2O_3 and Rb_2CO_3. Subsequently, the powders were mixed and grounded in a ball mill with stabilized zirconia balls, and calcined at 1773 K, for 20 h in air. The calcined powder was then planetary ball-milled with stabilized zirconia balls for 4 h, at 200 rpm and sieved to pass 325 mesh (45 μm).

Fig. 2 Crystal structure of an ABO_3 perovskite

Table 1 Compilation of experimentally determined RE-perovskite crystal structures

RE-perovskite-type oxides ABO_3	Crystal structure	Lattice parameters (Å)			References
		a	b	c	
$LaFeO_3$	Orthorhombic	5.5655	7.8383	5.5779	[39, 40]
$YFeO_3$	Orthorhombic	5.2819	5.5957	7.6046	[41, 42]
$PrFeO_3$	Orthorhombic	5.4820	5.5780	7.7860	[42, 43]
$LaNiO_3$	Rhombohedral	5.4574	–	13.146	[42, 44]
	Cubic	3.8400	3.8400	3.8400	[42, 45]
YVO_3	Orthorhombic	5.2772	5.6045	7.5729	[42, 46]
$EuAlO_3$	Orthorhombic	5.2891	7.466	5.2815	[42, 47]
$EuFeO_3$	Orthorhombic	5.3754	5.6015	7.6876	[42, 48]
$GdCrO_3$	Orthorhombic	5.3120	5.5140	7.6110	[42, 49]
	Rhombohedral	5.3150	–	7.6020	[42, 49]
$LaTiO_3$	Orthorhombic	5.6247	5.6071	7.9165	[42, 50]
$NdGaO_3$	Orthorhombic	5.4276	5.4979	7.7078	[42, 51]
$LaVO_3$	Orthorhombic	5.5552	5.5493	7.8432	[42, 52]
$LaAlO_3$	Rhombohedral	5.3642	–	13.108	[42, 53]
$NdAlO_3$	Rhombohedral	5.322	–	12.916	[42, 54]
$PrAlO_3$	Rhombohedral	5.333	–	12.984	[42, 55]
$CeFeO_3$	Rhombohedral	5.515	–	7.8150	[42, 56]
$GdAlO_3$	Rhombohedral	5.237	–	7.4435	[42, 57]
$La_{0.4}Sr_{0.6}FeO_3$	Rhombohedral	5.489	–	13.422	[58]

Alternatively, the glycine-nitrate route, also known as the combustion method, involves the use of nitrates instead of oxides as precursors, a dispersant (nitric or stearic acid) and fuel (glycine). These reagents are mixed in distilled water and heated until the excess free water evaporates. Subsequently, the resulting viscous liquid is auto-ignited by putting it in a preheated plate at a temperature around 673 K. Subsequently the as-burnt powder is calcined at a temperature typically around 1200 K for 3 to 5 h. This method has been reported in numerous studies involving RE-perovskite-type oxides for applications in Ni/MH batteries [27, 59, 64, 65]. For instance, Deng et al. [59] prepared RE-perovskite-type oxides to built-up electrodes for Ni/MH cells using the combustion method. They used stearic acid ($C_{17}H_{35}COOH$) as a dispersant, which was heated and melted. Stoichiometric amounts of $La(NO_3)_3 \cdot 6H_2O$, $Fe(NO_3)_3 \cdot 9H_2O$ and $Sr(NO_3)_2$ were added as precursors. The mixture was stirred by a magnetic mixer until a homogeneous solution was produced. The solution was ignited in air and the powders obtained were calcined at 1123 K for 3 h in a muffle furnace.

Sol–gel methods, especially, the well-known 'Pechini method', have been another option for the synthesis of perovskite-type oxides in previous studies [66, 67]. This method involves the mixing of perovskite precursors in nitrate and oxide form followed by the addition of a chelating agent, ethylene glycol as the sol-forming product,

desiccation and calcination. For example, Song et al. [67] prepared $LaCrO_3$ for Ni/MH batteries using the Pechini method. They used a mixture of $La(NO_3)_3 \cdot 6H_2O$, $Cr(NO_3)_3 \cdot 9H_2O$, citric acid, and ethylene glycol. These reagents were dissolved in distilled water to form an aqueous solution and then stirred in a water bath at 353 K until a gel was formed. The gel was then desiccated in a dying oven at 353 K for 24 h. The gel obtained was ground and calcined at 1073 K for 2 h to form the final powders.

Early studies have reported that the overall crystal structure of perovskite-type oxides is not affected by the synthesis method [68, 69]. However, changes in the crystal structure of perovskite-type oxides have been observed due to compositional variations, such as substituting the mean A-site ionic radius or the B-site [59]. Moreover, changes in the grain size have been observed depending on the synthesis route [68]. In this sense, the sol–gel method results in smaller grain sizes than the solid-state reaction method. In fact, the Pechini method is known for delivering homogeneous solutions with a great control of composition and production of ultrafine nanometric oxides [70, 71], which makes this method very attractive for recent developments and future trends in the field of Ni/MH batteries (see "Drawbacks and future challenges"). Compared with the solid-state reaction, the glycine-nitrate route and the sol–gel technique require lower calcination temperatures and reduced calcination times to yield pure crystals of

perovskite-type oxides. This fact results in energy-saving, which is also important in terms of cost reduction.

Performance and hydrogen absorption mechanisms of rare-earth perovskite-type electrode materials in Ni/MH batteries

RE-perovskite ABO_3 oxides are known to show catalytic behavior in hydrogen-rich media [72, 73], thus it is not a surprise that these materials can be useful for hydrogen storage. Their application to hydrogen batteries is based on the advantages shown in the catalysis and ionic conduction fields. These advantages can be summarized as (1) Wide variety of composition and constituent elements, keeping essentially the basic structure unchanged and cost of the compound as low as possible. (2) Valence, stoichiometry and vacancy can be varied widely, so enhancing their hydrogen absorption properties. (3) Thermal stability. (4) corrosion resistance in alkaline electrolyte [30, 74, 75]. Nevertheless, one of the weakest points of this technology with respect to the intermetallic-based one is the operating temperature range for hydrogen absorption, which is usually above room temperature.

Some efforts have been made to find out the performance of RE-perovskite-type oxides for hydrogen storage at room temperature. Sakaguchi et al. [76] have been pioneers in studying a RE-perovskite oxide ($SrCe_{0.95}Yb_{0.05}O_3$) for Ni/MH batteries. In their study, RE-perovskite-based electrodes were able to experience hydrogen absorption/desorption at room temperature. In a subsequent work, Esaka et al. [28] proposed another RE-perovskite-type oxide with composition $ACe_{1-x}M_xO_{3-d}$ (A = Sr or Ba, M = rare earth element). This composition was found to successfully store hydrogen in the bulk electrode and could experience electrochemical hydrogen charge and discharge at room temperature. Despite the successful results, the maximum capacity value of the $ACe_{1-x}M_xO_{3-d}$ composition was 119 mAhg^{-1} which is significantly lower than the capacity values reported for commercial AB$_5$ alloys at room temperature.

In the late 2000s, Deng et al. [59] also studied RE-perovskite-type oxides for hydrogen batteries. Interestingly, they reported that RE-perovskite-based electrodes with the composition $La_{1-x}Sr_xFeO_3$ (for X = 0.2 and 0.4) presented not only a dependency with respect to the temperature of the system, but also with respect to the initial crystalline structure (see Fig. 3). For instance, a rhombohedral structure (X = 0.4) was able to accept more hydrogen within its structure rather than an orthorhombic one (X = 0.2). As a result, the discharge capacity value of the rhombohedral structure was 77 mAhg^{-1} at room temperature, whereas the orthorhombic one presented a
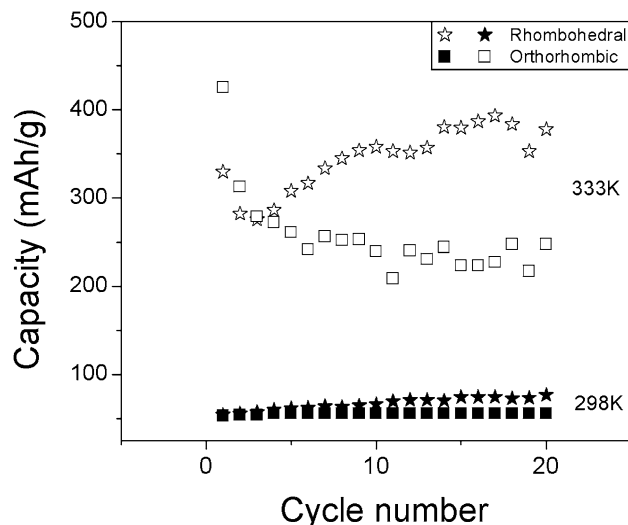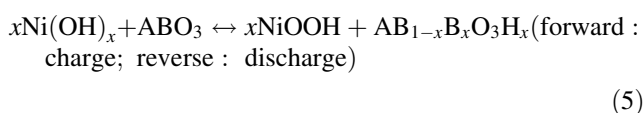

Fig. 3 Plot of the discharge capacity as a function of the cycle number in a $La_{1-x}Sr_xFeO_3$ ($x = 0.2$: orthorhombic structure, $x = 0.4$: rhombohedral structure). Data adapted from [59]

discharge capacity value of only 54 mAhg^{-1} at room temperature. These discharge capacity values were significantly improved at higher temperatures. In both cases, the average capacity values increased to 360 and 220 mAhg^{-1} for the rhombohedral and orthorhombic structures, respectively, at 333 K.

The electrochemical behavior of the RE-perovskite-type electrodes reported on the work of Deng et al. [59] can be attributed to the mechanisms for hydrogen absorption/desorption in RE-perovskite-type materials. The hydrogen absorption mechanism in RE-perovskite-type oxides is similar to that presented before for intermetallic alloys, where the storage of hydrogen atoms is given by the reduction of water at the interface electrolyte/active material. Hydrogen atoms are then captured within the structure of the RE-perovskite-type oxide to form a solid solution, i.e., a hydride compound [27, 59, 77]. Accordingly, the half-cell electrochemical reaction at the RE-perovskite-type negative electrode is:

$$ABO_3 + xH_2O + xe^- \leftrightarrow AB_{1-x}B_xO_3H_x \\ + xHO^- \text{(forward: charge; reverse: discharge)} \quad (4)$$
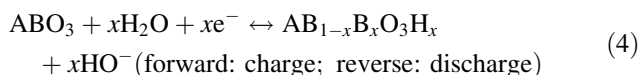
Thus, the overall reaction for the Ni/MH battery can be re-defined as follows:

$$xNi(OH)_x + ABO_3 \leftrightarrow xNiOOH + AB_{1-x}B_xO_3H_x \text{(forward : charge; reverse : discharge)} \quad (5)$$

Typical charge and discharge curves of the RE-perovskite-type electrodes show long and flat potential plateaus, Fig. 4a, b, which represents the interaction between hydrogen atoms and oxygen in the oxide during

the absorption/desorption process [27, 78]. In the charge process, the plateau is more notorious due to the formation of stable chemical bonds between protons and oxygen in the oxide. This plateau is affected by temperature. For instance, as the temperature increases from 298 to 333 K, the charge potential plateau tends to decrease, Fig. 4a [27, 59, 77, 78]. This phenomenon is associated with a decrease in electrode polarization when the temperature increases. Unlike the charge potential, the beginning of the discharge plateau remains almost unaltered with temperature, which yields an advantage over traditional AB_5 alloys, whose voltage plateau rises when the temperature increases and, therefore, might harm the properties of the cell, i.e., cause hydrogen recombination and irreversible electrolyte decomposition [79]. In addition to the potential value, the extent of the plateau and thus the
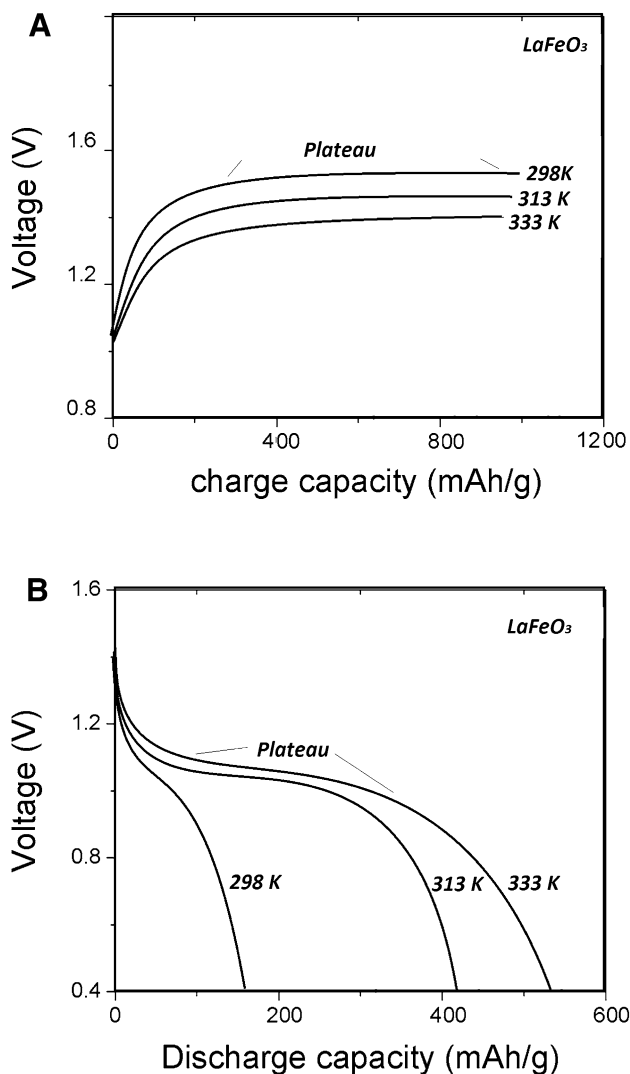
total discharge capacity increases when the temperature increases, Fig. 4b. This phenomenon is attributed to the mechanism of hydrogen ion migration in the unit cell of perovskite-type oxides. In these compounds, hydrogen atoms are inserted with the lattice oxygen, where it moves by cation hopping or jumping between immobile host oxygen ions. Alternatively, the protons can also move as a passenger on a larger ion like OH^- and H_3O^+ [80, 81]. At high temperatures, the phonons vibration as well as the cell expansion facilitates the movement of free H^+ ions. To some extent, it reduces the activation energy for H^+ ion diffusion and exhibits higher practical electrochemical capacities [82].

Interestingly, the combination of hydrogen absorption/ desorption and corrosion properties in RE-perovskite-type oxides provides them a great advantage over intermetallic-based ones. For example, intermetallic compounds show degradation in highly concentrated alkaline electrolytes which affects ionic conductivity and restricts the voltage window [83]. Instead, RE-perovskite-type oxides are able to operate at an increased concentration of electrolyte (OH^-) which benefits the electrochemical reaction. As a result, the discharge capacity of the RE-perovskite-type oxide electrode can increase with the rise of electrolyte concentration. This fact has been reported by Song et al. [84] using a $LaCrO_3$ composition as shown in Fig. 5. Similarly, the increment of the cell temperature is another factor that benefits the electrochemical reaction (see Figs. 4 and 5), leading to an improved discharge capacity as reported for different perovskite-type compositions [27, 59, 66, 77, 78]. These results show an advantage over intermetallic compounds whose electrochemical capacity is

Fig. 4 **a** Typical charge *curves* (at 125 mA/g) and **b** discharge *curves* (at 31.25 mA/g) of $LaFeO_3$ at various temperatures in a 7 M KOH solution. Data adapted from [78]
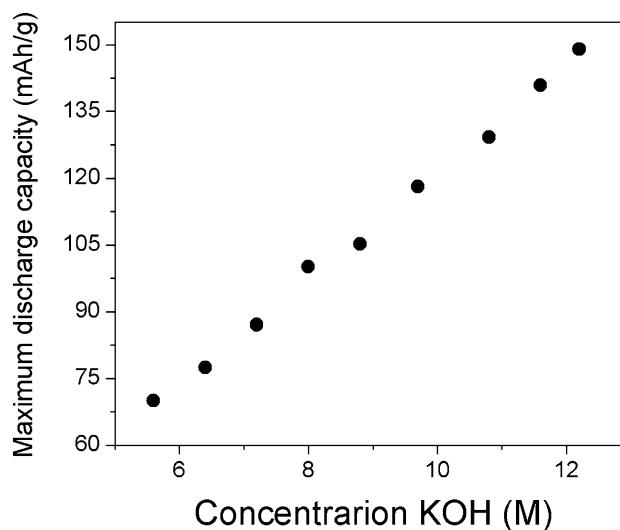

Fig. 5 Maximum discharge capacity as a function of the electrolyte concentration in a RE-perovskite $LaCrO_3$ at 298 K. Data adapted from [84]

affected by the increment of the operating temperature [85].

Table 2 summarizes the values of the electrochemical discharge capacity, hydrogen diffusion coefficient and the exchange current density for different perovskite-type electrodes reported in the literature. One can note from Table 2 that the values of the hydrogen diffusion coefficient of perovskite-type oxides remain lower than those values reported in the literature for conventional AB_5-type alloys, which are in the range from 10^{-6} to 10^{-11} cm/s^2 [86]. The values of the diffusion coefficient do not experience an important change when the temperature is increased. This fact reveals that the diffusion rate at the electrode/electrolyte interface depends mainly on structure and surface area. Among different RE-perovskite-type oxides, $LaFeO_3$ composition has exhibited considerable electrochemical capacity, ranging from 80 to 350 mAhg^{-1} at temperatures from 298 to 333 K, respectively. Using nanometric $LaFeO_3$ powders has resulted in an improvement of the electrochemical performance of this compound [64]. The improvement in the hydrogen diffusion coefficient and exchange current density (electro-catalytic activity of the charge transfer at the interface) of nanometric $LaFeO_3$ indicates that the nanometric particle size increases the surface area in contact with electrolyte and maximizes surface activity. Thus, the reaction kinetics is improved and consequently higher electrochemical capacity is obtained in comparison to the micrometric $LaFeO_3$ powder. It is worth mentioning that the exchange current density increases when the temperature increases, which confirms that the electro-catalytic activity of the charge transfer process increases as well.

The $LaCrO_3$ composition is also one of the promising perovskite-type electrodes presenting a good electrochemical capacity at 298 and at 333 K. It is worth mentioning that both $LaFeO_3$ and $LaCrO_3$ compositions present a sustainable stability without any crystal structure change in charge/discharge cycles (new phases are not formed after electrochemical cycling), see Fig. 6a, b. Interestingly, XRD patterns, like in Fig. 6, are typical of perovskite electrodes after galvanostatic charge/discharge cycling, which reveals the structural stability of these compounds during the hydrogen absorption/desorption process [27, 59, 66, 78]. Perovskite-type oxides present a small lattice expansion when compared with intermetallic alloys. For example, the $LaCrO_3$ composition has a volume change about 0.4% [67]. In contrast, the intermetallic alloy-$LaNi_5$ presents a volume change about 25% in each hydrogenation because of the introduction of H atoms in the interstices of the $CaCu_5$ structure [87]. Up to date, reported values of volume change for different perovskite-type oxides remains below 1% after hydrogenation [67, 77], which is significantly lower than values reported for traditional intermetallic alloys. This fact might result in an advantage for perovskite-type electrodes since they could be resistant to crack formation and spalling due to the lattice expansion during electrochemical cycling. In this sense, the few morphological studies about perovskite-type electrodes suggest that those are not free of damage after hydrogenation [66], Fig. 7. However, a systematic study combining XRD data (to calculate lattice parameters before and after electrochemical cycling) and SEM (to evaluate morphology after each hydrogenation) is highly recommended in future investigations to determine if the damage is attributed to the lattice expansion or to any other process.

Recently, another perovskite-type oxide, the $LaGaO_3$ compound, has been proposed for the negative electrode in Ni/MH batteries, Table 2. The $LaGaO_3$ consists of a single phase that crystallizes in an orthorhombic structure. This oxide first presents a discharge capacity with a maximum value of 220 mAhg^{-1} at 333 K, which decreases after the first three charge/discharge cycles [66, 88]. This degradation phenomenon with cycling has been observed as well in others RE-perovskite-type oxides [27]. The degradation of

Table 2 Compilation of experimentally determined discharge capacity, diffusion coefficient and exchange current density for different RE-perovskite-type electrodes

RE-perovskite-type oxides ABO_3	Steady discharge capacity (mAh/g) at 125 mA/g		Diffusion coefficient (D) (cm^2/s)		Exchange current density (I_o) (mA/g)		References
	298 K	333 K	298 K	333 K	298 K	333 K	
$LaFeO_3$	80	350	0.8×10^{-17}	4×10^{-17}	1.2	2.9	[78]
Nano-$LaFeO_3$	130	375	1.1×10^{-14}	2.9×10^{-14}	28	80	[64]
$LaCrO_3$	107	285	2.9×10^{-15}	*	38	*	[27, 67]
$LaGaO_3$	*	12	*	2.9×10^{-10}	*	70.6	[66]
$La_{0.8}Sr_{0.2}FeO_3$	50	230	1.6×10^{-17}	4×10^{-17}	37.8	83.2	[59]
$La_{0.6}Sr_{0.4}FeO_3$	70	350	0.8×10^{-17}	2×10^{-17}	42.8	78.3	[59]

* Data not availabe in the literature

cycling stability of RE-perovskite-type oxides has been explained by the corrosion behavior of the electrode because of the reduction in the electroactive surface area of
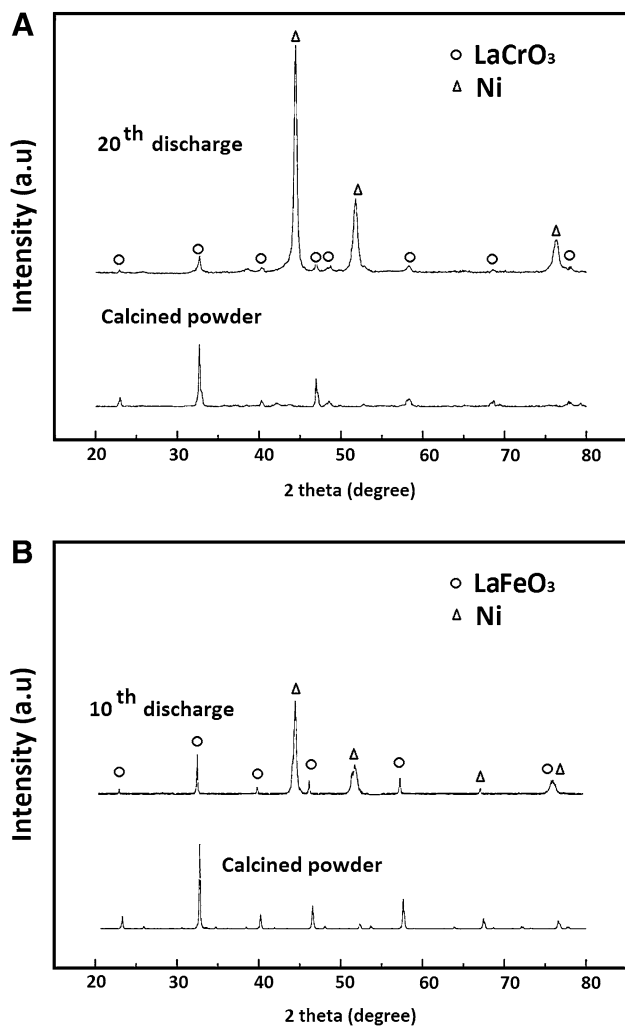

Fig. 6 XRD patterns of the calcined and discharged perovskite-type electrodes, **a** LaCrO₃ composition, **b** LaFeO₃ composition. Ni peaks correspond to the presence of nickel powder added as a binder. Data adapted from [27, 78]

the electrochemical reaction with cycling. Nevertheless, detailed research is still needed to understand the degradation phenomena during electrochemical cycling.

Therefore, it is clear that RE-perovskite-type oxides present electrochemical reversibility for hydrogen absorption/desorption in alkaline media and can be regarded as alternative negative electrode materials for hydrogen batteries. Although its performance is affected by the temperature of the system, this fact should not be considered as a disadvantage in terms of a possible real application in hydrogen batteries. Many of the intermetallic compounds suffer degradation of its electrochemical capacity when they are used at high temperature [89]. Instead, RE-perovskite-type electrodes can show very high capacities (over 400 mAhg^{-1}) at high temperatures, which could be extremely useful for example in high temperature Ni/MH secondary batteries. Nevertheless, Young et al. [83] in a recent study reported promising high capacity values (around 370 mAhg^{-1}) using perovskite electrodes at room temperature (the compositions have not yet been disclosed). Of course, there is still work to do in terms of exploring new compositions and solving some inherent drawbacks that can limit its application.

Drawbacks and future challenges

Currently, pending issues of RE-perovskite oxides for electrode materials are the focus of attention of researchers. These issues are mainly associated with the nature of the atomic interactions of perovskites. First, RE-perovskite-type oxides present a restricted exchange current density. This fact is attributed to the intrinsic conductivity of these materials which leads to the higher resistance during the charge transfer process. Second, RE perovskite type oxides have several times higher hydrogen diffusion coefficients than intermetallic alloys. Third, the degradation mechanisms of initial discharge capacity are not well understood. Accordingly, the improvement of charge transfer at the

Fig. 7 SEM micrograph of a LaGaO₃ electrode surface: **a** as-prepared electrode and **b** after 20th cycles. Reprinted from Ceramics International [66]
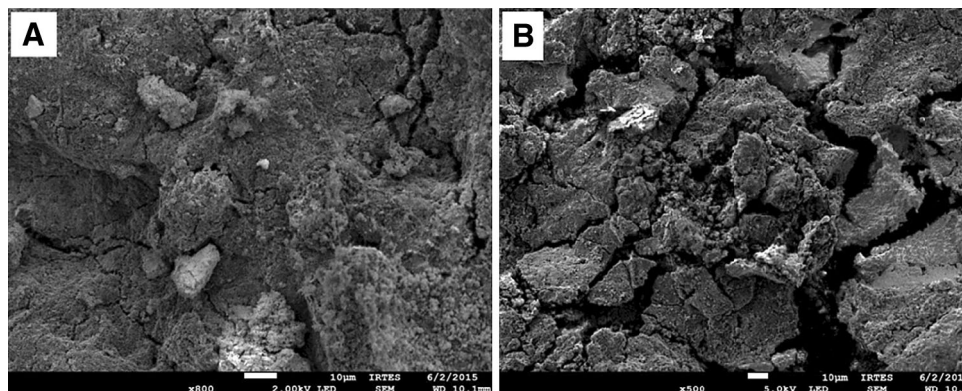
electrode/electrolyte interface and of the hydrogen mass transportation are key factors to achieve a better performance in hydrogen batteries. In this sense, recent studies have proposed nanosized RE-perovskite oxide particles for the production of negative electrodes on the basis that nanomaterials with high surface area could maximize the surface activity [64, 65]. As a result, nanosized RE-perovskite-type oxides should improve the reaction kinetics of electrode materials, and afford a shorter distance for ionic mass and charge transportation. In fact, experiments carried out with nanosized $LaFeO_3$ particles have shown an enhanced reaction kinetics, which facilitates the production of considerable higher specific capacities, see Table 2 [64]. It is worth noting that following this research line, the Pechini and combustion synthesis routes are regarded as the most appropriate techniques for the production of the nanosized active material rather than the solid-state production method (see "Synthesis of rare-earth perovskite-type oxides for applications in Ni/MH batteries").

Despite the improvement in the specific capacity using nanosized powders, the values of the hydrogen diffusion coefficient in RE-perovskite-type oxides are still lower than the diffusion values in hydrogen storage alloys. This fact has been attributed to the tendency of the nanosized powder to readily form aggregates, which limits the contact with the electrolyte, and consequently, hinders hydrogen diffusion [64]. As a result, investigations are currently focused on finding out new ways to improve ionic mass and charge transportation. One of the proposed solutions is substituting A or B sites in the ABO_3 formula to create vacancies and, therefore, to improve diffusion properties [63]. Of course, this solution should be also taken using nanosized powder, since doping is not enough by itself to decrease by itself the hydrogen diffusion coefficient close to the diffusion values in intermetallic alloys.

Another alternative for improving performance of RE-perovskite-type oxides in Ni/MH batteries is to prevent the aggregation of nanosized powders. The proposed solution consists of building up a coating on the surface of the oxide particles. An ideal coating for RE-perovskite-type oxides should possess multiple characteristics. For instance, it must help to avoid the aggregation of particles, be supportive in favor of hydrogen transfer, and provide protection against the alkaline electrolyte, especially at elevated temperatures. Recently, $LaFeO_3$ particles have been evenly coated with carbon and polyaniline (PANI) hybrid layers after carbon–PANI treatment [65]. The carbon layers prevent the nano-sized $LaFeO_3$ particles from aggregation. The PANI layers also enhance the electrocatalytic activity, facilitating hydrogen protons transferring from the electrolyte to the electrode interface. The cooperation of carbon and PANI hybrid layers results in a significant enhancement of the electrochemical performance at high

temperatures. At an elevated temperature (333 K), the maximum discharge capacity of the $LaFeO_3$ electrodes increases remarkably from 231 to 402 $mAhg^{-1}$, which is significantly higher than the capacity values reported for AB_5 intermetallic alloys. Of course, the improvement achieved using RE-perovskite-type electrodes has been obtained at higher temperatures (310–333 K). Thus, these findings are of particular interest for the development of the next generation of high performing and high temperature Ni/MH batteries.

Ni/MH batteries are often used at temperatures that rise well above room temperature, especially in fast-charge applications, and/or in hot environments [11]. For example, in certain electrical apparatus, it is necessary that the battery can be charged at lower current and under a relative high temperature environment (up to 373 K). Under such conditions, the normal Ni/MH batteries (owing to the limits of their structure) cannot be fully charged, and thus a decrease of discharge capacity occurs. Therefore, efforts are currently carried out to obtain RE-perovskite-type electrodes with a wide temperature operating range, in the expectation that these materials can ensure features such as high charge efficiency as well as prolonged cycle life and safety.

RE-perovskite-type oxides are also promising materials for hydrogen storage in other applications such as in fuel cells [90]. For example, the RE perovskite type oxide $LaFeO_3$ could easily absorb the proton primarily dissociated from water. As a result, unlike intermetallic alloys, RE-perovskite-type oxides like $LaFeO_3$ do not require being activated before charge/discharge operation in gas-/solid hydrogen storage applications [64]. This advantage should be exploited for its application in real devices. Future research should also be focused on new RE-perovskite-type compositions and new methods (surface and electrolyte modification, blended oxides) which can allow us to obtain better performance in Ni/MH batteries and/or in hydrogen storage devices.

Conclusions

Rare-earth perovskite ABO_3 type oxides for application in Ni/MH batteries have been reviewed. This review paper summarizes the efforts to improve the performance and expand the applicability of Ni/MH batteries undertaken by scientists in recent years. Rare earth perovskite-type oxides have attracted the attention of researchers as a promising option to compete against traditional intermetallic-base anodes in Ni/MH batteries due to its reversible electrochemical behavior, high natural abundance, facile synthesis, low price, and environmental benignity. Recent research works have shown that RE-perovskite-type oxides

present excellent discharge capacity at high temperatures, and consequently, are regarded as a prominent alternative for negative electrode materials for the next generation of high-temperature and high-performance Ni/MH batteries. Further research work is expected to optimize the properties and performance of these interesting compounds, not only for Ni/MH batteries but also for hydrogen storage devices.

Author contribution statement All the authors have made a significant contribution to the writing of this manuscript.

Compliance with ethical standards

Conflict of interest The authors declare no conflict of interests regarding the publication of this manuscript.

References

1. Young, K.H.: Research in nickel/metal hydride batteries. Batteries **2**(4), 31 (2016). doi:10.3390/batteries2040031
2. Tanabe, E.H., Schlemmer, D.F., Aguiar, M.L., Dotto, G.L., Bertuol, D.A.: Recovery of valuable materials from spent NIMH batteries using spouted bed elutriation. J. Environ. Manage. **171**, 177–183 (2016). doi:10.1016/j.jenvman.2016.02.011
3. Weiss, B., Obi, M.: Clean energy technology: investment and investment financing in renewable energy, batteries, energy supply and storage. In: Environmental Risk Mitigation, pp. 107–135. Springer, Berlin (2016). doi: 10.1007/978-3-319-33957-3_6
4. Aditya, J.P., Ferdowsi, M.: Comparison of NiMH and Li-ion batteries in automotive applications. In: Vehicle Power and Propulsion Conference, VPPC'08, IEEE, pp. 1–6, (2008). doi: 10.1109/VPPC.2008.4677500
5. Zhan, F., Jiang, L.J., Wu, B.R., Xia, Z.H., Wei, X.Y., Qin, G.R.: Characteristics of Ni/MH power batteries and its application to electric vehicles. J. Alloy. Compd. **293**, 804–808 (1999). doi:10.1016/S0925-8388(99)00361-8
6. Zhu, W.H., Zhu, Y., Davis, Z., Tatarchuk, B.J.: Energy efficiency and capacity retention of Ni–MH batteries for storage applications. Appl. Energy **106**, 307–313 (2013). doi:10.1016/j.apenergy.2012.12.025
7. Soria, M.L., Chacón, J., Hernández, J.C., Moreno, D., Ojeda, A.: Nickel metal hydride batteries for high power applications. J. Power Sources **96**(1), 68–75 (2001). doi:10.1016/S0378-7753(00)00677-7
8. Ouchi, T., Young, K.H., Moghe, D.: Reviews on the Japanese patent applications regarding nickel/metal hydride batteries. Batteries **2**(3), 21 (1999). doi:10.3390/batteries2030021
9. Barré, A., Deguilhem, B., Grolleau, S., Gérard, M., Suard, F., Riu, D.: A review on lithium-ion battery ageing mechanisms and estimations for automotive applications. J. Power Sources **241**, 680–689 (2013). doi:10.1016/j.jpowsour.2013.05.040
10. Chen, J., Bradhurst, D.H., Dou, S.X., Liu, H.K.: Nickel hydroxide as an active material for the positive electrode in rechargeable alkaline batteries. J. Electrochem. Soc. **146**(10), 3606–3612 (1999). doi:10.1149/1.1392522
11. Fetcenko, M.A., Ovshinsky, S.R., Reichman, B., Young, K., Fierro, C., Koch, J., Ouchi, T.: Recent advances in NiMH battery technology. J. Power Sources **165**(2), 544–551 (2007). doi:10.1016/j.jpowsour.2006.10.036
12. Sakintuna, B., Lamari-Darkrim, F., Hirscher, M.: Metal hydride materials for solid hydrogen storage: a review. Int. J. Hydrog. Energy **32**(9), 1121–1140 (2007). doi:10.1016/j.ijhydene.2006.11.022
13. Chang, S., Young, K.H., Nei, J., Fierro, C.: Reviews on the US patents regarding nickel/metal hydride batteries. Batteries **2**(2), 10 (2016). doi:10.3390/batteries2020010
14. Hong, K.: The development of hydrogen storage alloys and the progress of nickel hydride batteries. J. Alloy. Compd. **321**(2), 307–313 (2001). doi:10.1016/S0925-8388(01)00957-4
15. Zhao, X., Ma, L.: Recent progress in hydrogen storage alloys for nickel/metal hydride secondary batteries. Int. J. Hydrog. Energy **34**(11), 4788–4796 (2009). doi:10.1016/j.ijhydene.2009.03.023
16. Young, K.H., Yasuoka, S.: Capacity degradation mechanisms in nickel/metal hydride batteries. Batteries **2**(1), 3 (2016). doi:10.3390/batteries2010003
17. Khaldi, C., Lamloumi, J.: Electrochemical study of the cobalt-containing and non-cobalt-containing AB5 alloys used as negative electrodes in nickel–metal hydride batteries. In: Progress in Clean Energy. Springer, Berlin, (2015), (2):3–14. doi:10.1007/978-3-319-17031-2_1
18. Zhang, Y., Hou, Z., Cai, Y., Hu, F., Qi, Y., Zhao, D.: Electrochemical hydrogen storage behavior of as-cast and as-spun RE–Mg–Ni–Mn-based alloys applied to Ni–MH battery. Int. J. Mater. Res. **107**(9), 824–834 (2016). doi:10.3139/146.111412
19. Inoue, H., Kotani, N., Chiku, M., Higuchi, E.: Ti–V–Cr–Ni alloys as high capacity negative electrode active materials for use in nickel–metal hydride batteries. Int. J. Hydrog. Energy **41**(23), 9939–9947 (2016). doi:10.1016/j.ijhydene.2016.02.004
20. Liu, Y., Pan, H., Gao, M., Wang, Q.: Advanced hydrogen storage alloys for Ni/MH rechargeable batteries. J. Mater. Chem. **21**(13), 4743–4755 (2011). doi:10.1039/C0JM01921F
21. Belgacem, Y.B., Khaldi, C., Lamloumi, J., Takenouti, H.: The electrochemical performance of AB3-type hydrogen storage alloy as anode material for the nickel metal hydride accumulators. J. Solid State Electrochem. **20**(7), 1949–1959 (2016). doi:10.1007/s10008-016-3198-3
22. Norby, T., Widerøe, M., Glöckner, R., Larring, Y.: Hydrogen in oxides. Dalton Trans. **19**, 3012–3018 (2004). doi:10.1039/B403011G
23. Björketun, M.E., Sundell, P.G., Wahnström, G.: Structure and thermodynamic stability of hydrogen interstitials in $BaZrO_3$ perovskite oxide from density functional calculations. Faraday Discuss. **134**, 247–265 (2007). doi:10.1039/B602081J
24. Tsuchiya, B., Nagata, S., Toh, K., Shikama, T.: Effects of ion beam modification on absorption and transport of hydrogen in perovskite-type oxide ceramics. Nucl. Instrum. Methods Phys. Res. Sect. B **242**(1), 588–590 (2006). doi:10.1016/j.nimb.2005.08.076
25. Matsumoto, H., Shimura, T., Iwahara, H., Higuchi, T., Yashiro, K., Kaimai, A., Mizusaki, J.: Hydrogen separation using proton-

conducting perovskites. J. Alloy. Compd. **408**, 456–462 (2006). doi:10.1016/j.jallcom.2004.12.093

26. Orimo, S.I., Nakamori, Y., Eliseo, J.R., Züttel, A., Jensen, C.M.: Complex hydrides for hydrogen storage. Chem. Rev. **107**(10), 4111–4132 (2007). doi:10.1021/cr0501846

27. Deng, G., Chen, Y., Tao, M., Wu, C., Shen, X., Yang, H., Liu, M.: Study of the electrochemical hydrogen storage properties of the proton-conductive perovskite-type oxide LaCrO$_3$ as negative electrode for Ni/MH batteries. Electrochim. Acta **55**(3), 884–886 (2010). doi:10.1016/j.electacta.2009.09.078

28. Esaka, T., Sakaguchi, H., Kobayashi, S.: Hydrogen storage in proton-conductive perovskite-type oxides and their application to nickel–hydrogen batteries. Solid State Ionics **166**(3), 351–357 (2004). doi:10.1016/j.ssi.2003.11.023

29. Snaith, H.J.: Perovskites: the emergence of a new era for low-cost, high-efficiency solar cells. J. Phys. Chem. Lett. **4**(21), 3623–3630 (2013). doi:10.1021/jz4020162

30. Tejuca, L.G., Fierro J.L.G.: Properties and applications of perovskite-type oxides, 1st edn. In: Tejuca, L.G., Fierro J.L.G. (eds.), vol. 1, pp. 1–215. Marcel dekker Inc., New york (1993)

31. Rida, K., Benabbas, A., Bouremmad, F., Pena, M.A., Martinez-Arias, A.: Surface properties and catalytic performance of La$_{1-x}$Sr$_x$CrO$_3$ perovskite-type oxides for CO and C$_3$H$_6$ combustion. Catal. Commun. **7**, 963–968 (2006). doi:10.1016/j.catcom.2006.04.011

32. Grabowska, E.: Selected perovskite oxides: characterization, preparation and photocatalytic properties—a review. Appl. Catal. B **186**, 97–126 (2016). doi:10.1016/j.apcatb.2015.12.035

33. Chen, L., Pradhan, S.: Low temperature synthesis of metal doped perovskites catalyst for hydrogen production by auto-thermal reforming of methane. Int. J. Hydrog. Energy **41**(33), 14605–14614 (2016). doi:10.1016/j.ijhydene.2016.06.235

34. Medarde, M.L.: Structural, magnetic and electronic properties of perovskites (R = rare earth). J. Phys.: Condens. Matter **9**(8), 1679–1707 (1997). doi:10.1088/0953-8984/9/8/003

35. Bednorz, J.G., Müller, K.A.: Perovskite-type oxides—the new approach to high-Tc superconductivity. Rev. Mod. Phys. **60**(3), 585 (1988). doi:10.1103/RevModPhys.60.585

36. Galasso, F.S.: Structure, properties and preparation of perovskite-type compounds, 1st ed. In: Galaso, F. (eds.) vol. 5, pp. 140–144. Pergamon Press Ltd., New york (1969)

37. Tanaka, H., Misono, M.: Advances in designing perovskite catalysts. Curr. Opin. Solid State Mater. Sci. **5**(5), 381–387 (2001). doi:10.1016/S1359-0286(01)00035-3

38. Shi, J., Guo, L.: ABO3-based photocatalysts for water splitting. Progr. Nat. Sci.: Mater. Int. 22, 592–615 (2012). doi:10.1016/j.pnsc.2012.12.002

39. Thirumalairajan, S., Girija, K., Hebalkar, N.Y., Mangalaraj, D., Viswanathan, C., Ponpandian, N.: Shape evolution of perovskite LaFeO$_3$ nanostructures: a systematic investigation of growth mechanism, properties and morphology dependent photocatalytic activities. RSC Adv. **3**, 7549–7561 (2013). doi:10.1039/C3RA00006K

40. Thirumalairajan, S., Girija, K., Hebalkar, N.Y., Mangalaraj, D., Viswanathan, C., Ponpandian, N.: Controlled synthesis of perovskite LaFeO$_3$ microsphere composed of nanoparticles via self-assembly process and their associated photocatalytic activity. Chem. Eng. J. **209**, 420–428 (2012). doi:10.1021/am503318y

41. Tang, P., Chen, H., Cao, F., Pan, G.: Magnetically recoverable and visible-light-driven nanocrystalline YFeO$_3$ photocatalysts. Catal. Sci. Technol. **1**, 1145–1148 (2011). doi:10.1039/C1CY00199J

42. Villars, P. (ed.): Inorganic solid phases, Springer Materials (online database). Springer, Heidelberg. http://materials.springer.com/isp/crystallographic/docs (2016). Accessed 14 March 2017

43. Tijare, S., Bakardjieva, S., Subrt, J., Joshi, M., Rayalu, S., Hishita, S., Labhsetwar, N.: Synthesis and visible light photocatalytic activity of nanocrystalline PrFeO$_3$ perovskite for hydrogen generation in ethanol–water system. Chem. Sci. **126**, 517–525 (2014). doi:10.1007/s12039-014-0596-x

44. Li, Y., Yao, S., Wen, W., Xue, L., Yan, Y.: Sol–gel combustion synthesis and visible-light-driven photocatalytic property of perovskite LaNiO3. J. Alloy. Compd. **491**(1), 560–564 (2010). doi:10.1016/j.jallcom.2009.10.269

45. Aman, D., Zaki, T., Mikhail, S., Selim, S.A.: Synthesis of a perovskite LaNiO3 nanocatalyst at a low temperature using single reverse microemulsion. Catal. Today **164**(1), 209–213 (2011). doi:10.1016/j.cattod.2010.11.034

46. Tsvetkov, A.A., Mena, F.P., Van Loosdrecht, P.H.M., Van Der Marel, D., Ren, Y., Nugroho, A., Sawatzky, G.A.: Structural, electronic, and magneto-optical properties of YVO3. Phys. Rev. B, **69**(7), 075110-1–075110-11 (2004). doi:10.1103/PhysRevB.69.075110

47. Garskaite, E., Sakirzanovas, S., Kareiva, A., Glaser, J., Meyer, H.: Synthesis and structure of europium aluminium garnet (EAG). Zeitschrift für anorganische und allgemeine Chemie **633**(7), 990–993 (2007). doi:10.1002/zaac.200700027

48. Li, S.Z., Huang, Y.J., Zhu, J.B., Zhang, Y., Chen, N., Hsia, Y.F.: XRD and Mössbauer investigation of phase segregation in Eu$_{1-x}$Sr$_x$FeO$_3$. Physica B **393**(1), 100–104 (2007). doi:10.1016/j.physb.2006.12.077

49. Cheng, Z., Wang, X., Dou, S.X., Kimura, H., Ozawa, K.: A novel multiferroic system: rare earth chromates. J. Appl. Phys. **107**, 900–905 (2010). doi:10.1063/1.3360358

50. Cwik, M., Lorenz, T., Baier, J., Müller, R., André, G., Bourée, F., Braden, M.: Crystal and magnetic structure of LaTiO$_3$: evidence for nondegenerate orbitals. Phys. Rev B **68**(6), 060401 (2003). doi:10.1103/PhysRevB.68.060401

51. Vasylechko, L., Akselrud, L., Morgenroth, W., Bismayer, U., Matkovskii, A., Savytskii, D.: The crystal structure of NdGaO3 at 100 and 293 K based on synchrotron data. J. Alloy. Compd. **297**(1), 46–52 (2000). doi:10.1016/S0925-8388(99)00603-9

52. Martínez-Lopez, M.J., Alonso, J.A., Retuerto, M., Fernández-Díaz, M.T.: Evolution of the crystal structure of RVO$_3$ (R = La, Ce, Pr, Nd, Tb, Ho, Er, Tm, Yb, Lu, Y) perovskites from neutron powder diffraction data. Inorg. Chem. **47**(7), 2634–2640 (2008). doi:10.1021/ic701969q

53. Luo, X., Wang, B.: Structural and elastic properties of LaAlO$_3$ from first-principles calculations. J. Appl. Phys. **104**(7), 73518-1–73518-7 (2008). doi: 10.1063/1.2990068

54. Ishihara, T., Matsuda, H., Mizuhara, Y., Takita, Y.: Improved oxygen ion conductivity of NdAlO3 perovskite-type oxide by doping with Ga. Solid State Ionics **70**, 234–238 (1994). doi:10.1016/0167-2738(94)90316-6

55. Moussa, S.M., Kennedy, B.J., Hunter, B.A., Howard, C.J., Vogt, T.: Low temperature structural studies on PrAlO3. J. Phys.: Condens. Matter **13**(9), L203–L209 (2001). doi:10.1088/0953-8984/13/9/102

56. Robbins, M., Wertheim, G.K., Menth, A., Sherwood, R.C.: Preparation and properties of polycrystalline cerium orthoferrite (CeFeO$_3$). J. Phys. Chem. Solids **30**(7), 1823–1825 (1969). doi:10.1016/0022-3697(69)90250-9

57. Raju, G.S.R., Park, J.Y., Jung, H.C., Moon, B.K., Jeong, J.H., Kim, J.H.: Luminescence properties of Dy 3+: GdAlO$_3$ nanopowder phosphors. Curr. Appl. Phys. **9**(2), e92–e95 (2009). doi:10.1016/j.cap.2008.12.037

58. Fossdal, A., Menon, M., Wærnhus, I., Wiik, K., Einarsrud, M.A., Grande, T.: Crystal structure and thermal expansion of La$_{1-x}$Sr$_x$FeO$_{3-\delta}$ materials. J. Am. Ceram. Soc. **87**(10), 1952–1958 (2004). doi:10.1111/j.1151-2916.2004.tb06346.x

59. Deng, G., Chen, Y., Tao, M., Wu, C., Shen, X., Yang, H.: Electrochemical properties of La$_{1-x}$Sr$_x$FeO$_3$ ($x = 0.2, 0.4$) as negative electrode of Ni–MH batteries. Electrochim. Acta **54**(15), 3910–3914 (2009). doi:10.1016/j.electacta.2009.02.007

60. Li, H.L., Liu, X.J., Huang, L.P.: Fabrication of transparent cerium-doped lutetium aluminum garnet (LuAG: Ce) ceramics by a solid-state reaction method. J. Am. Ceram. Soc. **88**(11), 3226–3228 (2005). doi:10.1111/j.1551-2916.2005.00554.x

61. Chandarak, S., Unruan, M., Sareein, T., Ngamjarurojana, A., Maensiri, S., Laoratanakul, P., Yimnirun, R.: Fabrication and characterization of $(1 − x)$ BiFeO3-xBaTiO3 ceramics prepared by a solid state reaction method. J. Magn **14**(3), 120–123 (2009). doi:10.4283/JMAG.2009.14.3.120

62. Li, C.Q., Zuo, H.B., Zhang, M.F., Han, J.C., Meng, S.H.: Fabrication of transparent YAG ceramics by traditional solid-state-reaction method. Trans. Nonferrous Metals Soc. China **17**(1), 148–153 (2007). doi:10.1016/S1003-6326(07)60064-8

63. Lim, D.K., Lee, K.C., Park, C.N, Song, S.J.: Preparation and hydrogen storage properties of BaZr0. 65Ce0.2Y0.1Rb0.05O3-δ as the negative electrode of a hydrogen battery. J. Ceram. Process. Res. **13**(3), 315–318 (2012), WOS:000306164500025

64. Wang, Q., Deng, G., Chen, Z., Chen, Y., Cheng, N.: Electrochemical hydrogen property improved in nano-structured perovskite oxide LaFeO$_3$ for Ni/MH battery. J. Appl. Phys. **113**(5), 053305-1-5 (2013). doi:10.1063/1.4790488

65. Pei, Y., Du, W., Li, Y., Shen, W., Wang, Y., Yang, S., Han, S.: The effect of carbon–polyaniline hybrid coating on high-temperature electrochemical performance of perovskite-type oxide LaFeO3 for MH–Ni batteries. Phys. Chem. Chem. Phys. **17**(27), 18185–18192 (2015). doi:10.1039/C5CP02395E

66. Kaabi, A., Tliha, M., Dhahri, A., Khaldi, C., Lamloumi, J.: Study of electrochemical performances of perovskite-type oxide LaGaO3 for application as a novel anode material for Ni–MH secondary batteries. Ceram. Int. **42**(10), 11682–11686 (2016). doi:10.1016/j.ceramint.2016.04.082

67. Song, M., Chen, Y., Tao, M., Wu, C., Zhu, D., Yang, H.: Some factors affecting the electrochemical performances of LaCrO$_3$ as negative electrodes for Ni/MH batteries. Electrochim. Acta **55**(9), 3103–3108 (2010). doi:10.1016/j.electacta.2010.01.030

68. Ecija, A., Larrañaga, A., Vidal, K., Ortega, L., Arriortua, M.I.: Synthetic methods for perovskite materials; structure and morphology. INTECH Open Access Publisher. Available online: http://cdn.intechopen.com/ (2012). Accessed on 6 Dec 2016)

69. Nakayama, S.: LaFeO$_3$ perovskite-type oxide prepared by oxide-mixing, co-precipitation and complex synthesis methods. J. Mater. Sci. **36**(23), 5643–5648 (2001). doi:10.1023/A:1012526018348

70. Derakhshi, Z., Tamizifar, M., Arzani, K., Baghshahi, S.: Synthesis and Characterization of LaCoxFe$_1$-xO$_3$ ($0 \le x \le 1$) Nano-Crystal Powders by Pechini Type Sol-Gel Method, Synthesis and Reactivity in Inorganic. Metal-Organic, and Nano-Metal Chem. **46**(1), 25–30 (2016). doi:10.1080/15533174.2014.900628

71. Chang, Y.S., Huang, F.M., Tsai, Y.Y., Teoh, L.G.: Synthesis and photoluminescent properties of YVO4: Eu 3+ nano-crystal phosphor prepared by Pechini process. J. Lumin. **129**(10), 1181–1185 (2009). doi:10.1016/j.jlumin.2009.05.020

72. Lee, Y.N., Lago, R.M., Fierro, J.L.G., González, J.: Hydrogen peroxide decomposition over Ln$_1$–xAxMnO$_3$ (Ln = La or Nd and A = K or Sr) perovskites. Appl. Catal. A **215**(1), 245–256 (2001). doi:10.1016/S0926-860X(01)00536-1

73. Tijare, S.N., Joshi, M.V., Padole, P.S., Mangrulkar, P.A., Rayalu, S.S., Labhsetwar, N.K.: Photocatalytic hydrogen generation through water splitting on nano-crystalline LaFeO$_3$ perovskite. Int. J. Hydrog. Energy **37**(13), 10451–10456 (2012). doi:10.1016/j.ijhydene.2012.01.120

74. Cimino, S., Pirone, R., Russo, G.: Thermal stability of perovskite-based monolithic reactors in the catalytic combustion of methane. Ind. Eng. Chem. Res. **40**(1), 80–85 (2001). doi:10.1021/ie000392i

75. Frangini, S., Masci, A., Zaza, F.: Molten salt synthesis of perovskite conversion coatings: a novel approach for corrosion protection of stainless steels in molten carbonate fuel cells. Corros. Sci. **53**(8), 2539–2548 (2011). doi:10.1016/j.corsci.2011.04.011

76. Sakaguchi, H., Hatakeyama, K., Kobayashi, S.S., Esaka, T.: Hydrogenation characteristics of the proton conducting oxide–hydrogen storage alloy composite. Mater. Res. Bull. **37**(9), 1547–1556 (2002). doi:10.1016/S0025-5408(02)00846-2

77. Deng, G., Chen, Y., Tao, M., Wu, C., Shen, X., Yang, H., Liu, M.: Preparation and electrochemical properties of La0.4Sr0.6FeO$_3$ as negative electrode of Ni/MH batteries. Int. J. Hydrog. Energy **34**(13), 5568–5573 (2009). doi:10.1016/j.ijhydene.2009.04.061

78. Deng, G., Chen, Y., Tao, M., Wu, C., Shen, X., Yang, H., Liu, M.: Electrochemical properties and hydrogen storage mechanism of perovskite-type oxide LaFeO$_3$ as a negative electrode for Ni/MH batteries. Electrochim. Acta **55**(3), 1120–1124 (2010). doi:10.1016/j.electacta.2009.09.078

79. Raju, M., Ananth, M.V., Vijayaraghavan, L.: Influence of temperature on the electrochemical characteristics of MmNi 3.03 Si 0.85 Co 0.60 Mn 0.31 Al 0.08 hydrogen storage alloys. J. Power Sources **180**(2), 830–835 (2008). doi:10.1016/j.jpowsour.2008.02.061

80. Nieto, S., Polanco, R., Roque-Malherbe, R.: Absorption kinetics of hydrogen in nanocrystals of BaCe0. 95Yb0. 05O3-δ proton-conducting perovskite. J. Phys. Chem. C **111**(6), 2809–2818 (2007). doi:10.1021/jp067389i

81. Jones, C.Y., Wu, J., Li, L., Haile, S.M.: Hydrogen content in doped and undoped BaPrO$_3$ and BaCeO$_3$ by cold neutron prompt-gamma activation analysis. J. Appl. Phys. **97**(11), 114908 (2005). doi:10.1063/1.1922590

82. Wang, Q., Chen, Z., Chen, Y., Cheng, N., Hui, Q.: Hydrogen storage in perovskite-type oxides ABO3 for Ni/MH battery applications: a density functional investigation. Ind. Eng. Chem. Res. **51**(37), 11821–11827 (2011). doi:10.1021/ie202284z

83. Young, K.H., Ng, K.Y., Bendersky, L.A.: A technical report of the robust affordable next generation energy storage system-BASF program. Batteries **2**(1), 2 (2016). doi:10.3390/batteries2010002

84. Song, M., Chen, Y., Tao, M., Wu, C., Zhu, D., Yang, H.: Some factors affecting the electrochemical performances of LaCrO$_3$ as negative electrodes for Ni/MH batteries. Electrochim. Acta **55**(9), 3103–3108 (2010). doi:10.1016/j.electacta.2010.01.030

85. Zhang, X., Chai, Y., Yin, W., Zhao, M.: Crystal structure and electrochemical properties of rare earth non-stoichiometric AB 5-type alloy as negative electrode material in Ni–MH battery. J. Solid State Chem. **177**(7), 2373–2377 (2004). doi:10.1016/j.jssc.2004.03.018

86. Kleperis, J., Wójcik, G., Czerwinski, A., Skowronski, J., Kopczyk, M., Beltowska-Brzezinska, M.: Electrochemical behavior of metal hydrides. J. Solid State Electrochem. **5**(4), 229–249 (2001). doi:10.1007/s100080000149

87. Sakai, T., Oguro, K., Miyamura, H., Kuriyama, N., Kato, A., Ishikawa, H., Iwakura, C.: Some factors affecting the cycle lives of LaNi$_5$-based alloy electrodes of hydrogen batteries. J. Less Common Met. **161**(2), 193–202 (1990). doi:10.1016/0022-5088(90)90027-H

88. Kaabi, A., Tliha, M., Dhahri, A., Khaldi, C., Lamloumi, J.: Electrochemical properties of the LaGaO$_3$ perovskite-type oxide used as negative electrode in Ni/MH accumulators. In: 7th

International Renewable Energy Congress (IREC), 1–5, (2016). doi:10.1109/IREC.2016.7478911

89. Young, K.H., Yasuoka, S.: Capacity degradation mechanisms in nickel/metal hydride batteries. Batteries **2**(1), 3 (2016). doi:10.3390/batteries2010003

90. Lototskyy, M., Tolj, I., Davids, M.W., Bujlo, P., Smith, F., Pollet, B.G.: Distributed hybrid MH–CGH$_2$ system for hydrogen storage and its supply to LT PEMFC power modules. J. Alloy. Compd. **645**, S329–S333 (2015). doi:10.1016/j.jallcom.2014.12.147